

## A Dwarf Transitional Protoplanetary Disk around XZ Tau B

Mayra Osorio<sup>1</sup>, Enrique Macías<sup>1</sup>, Guillem Anglada<sup>1</sup>, Carlos Carrasco-González<sup>2</sup>, Roberto Galván-Madrid<sup>2</sup>, Luis Zapata<sup>2</sup>, Nuria Calvet<sup>3</sup>, José F. Gómez<sup>1</sup>, Erick Nagel<sup>4</sup>, Luis F. Rodríguez<sup>2</sup>, José M. Torrelles<sup>5†</sup>, Zhaohuan Zhu<sup>6</sup>

### ABSTRACT

We report the discovery of a dwarf protoplanetary disk around the star XZ Tau B that shows all the features of a classical transitional disk but on a much smaller scale. The disk has been imaged with the Atacama Large Millimeter/Submillimeter Array (ALMA), revealing that its dust emission has a quite small radius of  $\sim 3.4$  au and presents a central cavity of  $\sim 1.3$  au in radius that we attribute to clearing by a compact system of orbiting (proto)planets. Given the very small radii involved, evolution is expected to be much faster in this disk (observable changes in a few months) than in classical disks (observable changes requiring decades) and easy to monitor with observations in the near future. From our modeling we estimate that the mass of the disk is large enough to form a compact planetary system.

*Subject headings:* planet-disk interactions — protoplanetary disks — stars: formation — stars: individual (XZ Tau B) — stars: pre-main sequence

---

<sup>1</sup>Instituto de Astrofísica de Andalucía (CSIC), Glorieta de la Astronomía s/n, E-18008 Granada, Spain; email: osorio@iaa.es

<sup>2</sup>Instituto de Radioastronomía y Astrofísica UNAM, Apartado Postal 3-72 (Xangari), 58089 Morelia, Michoacán, Mexico

<sup>3</sup>Department of Astronomy, University of Michigan, 825 Dennison Building, 500 Church St, Ann Arbor, MI 48109, USA

<sup>4</sup>Departamento de Astronomía, Universidad de Guanajuato, Guanajuato, Gto 36240, Mexico

<sup>5</sup>Institut de Ciències de l'Espai (CSIC)-Institut de Ciències del Cosmos (UB)/IEEC, Martí i Franquès 1, E-08028 Barcelona, Spain

<sup>6</sup>Department of Astrophysical Sciences, Princeton University, Princeton, NJ 08544, USA

†The ICC (UB) is a CSIC-Associated Unit through the ICE

## 1. Introduction

Planetary systems originate from the evolution of accretion disks of gas and dust that develop around young stars as part of the star formation process itself (Blum & Wurm 2008). However, the details of how planets form are far from well understood. Some accretion disks, known as “transitional disks” (Calvet et al. 2005), present central cavities and annular gaps in their dust emission that have been attributed to the effects of tidal interactions of orbiting planetary or protoplanetary bodies (Papaloizou et al. 2007, Zhu et al. 2011, Andrews et al. 2011, Osorio et al. 2014) and are considered signposts of the planet formation process. Typical transitional disks imaged so far have radii of 50-100 au and masses of 10-100  $M_J$ , with central cavities of 15-70 au in radius (Andrews et al. 2011, Espaillat et al. 2014, Andrews 2015). Nevertheless, some results, based on the spectral energy distribution (SED) modeling, suggest that significantly smaller disks should exist (McClure et al. 2008, Piétu et al. 2014), but direct imaging has not been possible yet.

XZ Tau B is a young M2 dwarf star (see stellar properties in Table 1) in the L1551 molecular cloud. It belongs to a triple system composed of the close pair XZ Tau A/C (separation  $\sim 0.09''$ ) and XZ Tau B (currently located  $\sim 0.3''$  to the NW; Carrasco-González et al. 2009). A sequence of expanding bubbles imaged by the HST (Krist et al. 2008) has been attributed to XZ Tau A/C (Carrasco-González et al. 2009, Zapata et al. 2015), while high velocity jets have been associated with both XZ Tau A/C and XZ Tau B (Krist et al. 2008).

During the Long Baseline Campaign of the ALMA Science Verification process, a field centered on HL Tau was observed at 2.9 mm and 1.3 mm (ALMA Partnership et al. 2015a, 2015b; hereafter AP2015a, AP2015b). XZ Tau B was reported only as an unresolved continuum source at 2.9 mm. Here we present a detailed analysis of the 1.3 mm continuum observations that angularly resolve the source.

## 2. Observations

The observations were carried out between 2014 October 14 and November 14 using 42 antennas of ALMA, with baselines from 12 to 15,240 m. The phase center was at the position of HL Tau,  $\alpha(\text{J2000})=4^{\text{h}}31^{\text{m}}38.4263^{\text{s}}$ ,  $\delta(\text{J2000})=18^{\circ}13'57.047''$ . The 1.3 mm data were obtained from 2014 October 24 to 31 with the ALMA correlator configured in 4 spectral windows of 2000 MHz and 128 channels each. The 2.9 mm data were obtained using wide spectral windows for the continuum and narrow spectral windows centered on the  $\text{HCO}^+(1-0)$ ,  $\text{HCN}(1-0)$ ,  $\text{CO}(1-0)$ , and  $\text{CN}(1-0)$  lines. A description of the observational setup and the

calibration process is given in AP2015a, AP2015b.

The continuum emission at 2.9 mm was imaged by AP2015a (beam =  $0.085'' \times 0.061''$ , PA= $-179^\circ$ ; rms =  $24 \mu\text{Jy beam}^{-1}$ ). We obtained cleaned, continuum subtracted, channel maps (channel width =  $0.25 \text{ km s}^{-1}$ ; beam =  $0.10'' \times 0.06''$ , PA= $12^\circ$ ) for the observed line transitions. No line emission was detected towards XZ Tau.

Images at 1.3 mm were obtained with the task *clean* of CASA (version 4.2.2). XZ Tau falls  $\sim 24''$  away from the phase center, where the response of the primary beam (FWHM  $\simeq 27''$  at 1.3 mm) is only 1/19. However, the extraordinary sensitivity of ALMA allows a good signal-to-noise imaging. To avoid HL Tau sidelobes in the XZ Tau field, we first cleaned the HL Tau emission and subtracted it from the uv data. We tried several self-calibration strategies. Although self-calibration improves slightly the images of HL Tau, it blurs the XZ Tau images. We attribute these unfavorable effects on XZ Tau to the lack of a strong compact source in the field and to the large separation of XZ Tau from the phase center. Since we are interested in XZ Tau, we did not apply self-calibration in our final images. Given the narrow channel width and small integration time per visibility, the expected bandwidth and time smearing are negligible at the position of XZ Tau ( $0.0016''$  and  $0.0035''$ , respectively).

Figure 1a shows our primary-beam corrected 1.3 mm image of XZ Tau B. The source is angularly resolved, with a size of  $\sim 0.05''$  and a flux density of  $7 \pm 2 \text{ mJy}^1$ . At 2.9 mm it was reported as angularly unresolved (size  $< 0.054''$ ) with a flux density of  $1.83 \pm 0.12 \text{ mJy}$  (AP2015a; Zapata et al. 2015). Uncertainties in flux densities have been calculated as in AP2015a, but adding quadratically the absolute flux density calibration uncertainty (5%) and the primary beam response uncertainty due to pointing errors ( $\sim 0.6''$ ), using the Dzib et al. (2014) prescription.

Since the 2.9 mm observations are less affected by the primary beam attenuation, they are much more sensitive. The fact that the source size upper limit set by these observations is similar to the observed size at 1.3 mm ( $\sim 0.05'' \simeq 7 \text{ au}$ ) indicates that the sensitivity of the 1.3 mm image is high enough to reveal the full structure of the source and not just the brightest part. Thus, we interpret the observed emission as tracing the dust of a very small ( $\sim 3.5 \text{ au}$  in radius) circumstellar disk.

Interestingly, the 1.3 mm ALMA image reveals substructure in the disk (Fig. 1a). Emission decreases towards the center, indicating a hole or cavity. Otherwise, the emission would peak towards the central position. We have plotted the real component of the visibility profile (Fig. 1b), which shows the characteristic null and negative region that confirm the

---

<sup>1</sup>Measured in a natural-weight image

presence of a central hole in the disk (e.g., Andrews et al. 2009). The null falls around 5-8  $M\lambda$ , corresponding to hole radii of 0.6-0.9 au to 1.4-2.2 au for the extreme cases of an infinite disk and a thin ring, respectively (Hughes et al. 2007)<sup>2</sup>. Since our small disk should be something intermediate, we estimate a radius of the hole  $\sim 1$  au, consistent with the value obtained from our modeling of the SED and image (§3). Thus, XZ Tau B appears to be a “transitional disk” (Calvet et al. 2005) with a small central cavity probably due to the tidal forces created by an orbiting substellar object or protoplanet (Andrews et al. 2011). In order to substantiate this interpretation we carried out a detailed modeling.

### 3. Modeling

The disk parameters are determined by modeling and fitting the observed SED and the normalized radial intensity profile of the 1.3 mm image. To construct the observed SED we compiled photometric and spectroscopic data from the Spitzer, WISE, Akari, and IRAS databases, from the literature (Hartigan & Kenyon 2003, White & Ghez 2001, Carrasco-González et al. 2009, AP2015a, Forgan et al. 2014), and from this paper. Measurements that do not separate the A and B components have been taken as upper limits.

Our model includes the contributions from both the central star and the disk. Since the XZ Tau B star is known to be optically variable (Sandell & Aspin 1998), we reanalyzed the results of Hartigan & Kenyon (2003) but using the photometry of XZ Tau A from Coffey et al. (2004) to estimate the aperture correction. The stellar and accretion (veiling) luminosities of XZ Tau B were obtained following Pecaut & Mamajek (2013), Kenyon & Hartmann (1995), and Calvet & Gullbring (1998) assuming an M2 star and an 8000 K blackbody as the veiling source. Finally, using the Siess et al. (2000) tracks, the stellar parameters were derived (Table 1). The contribution of the central star to the SED (Fig. 3a) is calculated by using the reanalyzed fluxes and extrapolating to other wavelengths following Kenyon & Hartmann (1995) and Pecaut & Mamajek (2013).

The disk is modeled using an updated version of the irradiated  $\alpha$ -accretion disk models with dust settling developed by D’Alessio et al. (2006). A dust grain population similar to the interstellar medium is used in the upper layers of the disk, while in the mid-plane a population of larger dust grains, with radii up to 1 mm, is assumed. The grain mixture composition is the same as in Osorio et al. (2014), but incorporating water ice with the abundance given by McClure et al. (2015), resulting in a dust-to-gas ratio of 0.0085. A

---

<sup>2</sup>Visibilities have been recentered on XZ Tau B, but not deprojected to account for the disk inclination. So, these values are only rough estimates

central cavity is included in the model by emptying the innermost regions of the disk. The edge of this region, or wall, is directly irradiated by the star and the accretion shock and, thus, heated to a higher temperature (D’Alessio et al 2005).

The high H, K, and L band fluxes (Hioki et al. 2009, White & Ghez 2001) indicate that hot dust, that may correspond to a residual inner disk, is present inside the cavity, suggesting that XZ Tau B is at an earlier pre-transitional stage (Espaillat et al. 2008). However, because of the variability of the star and the limited data in this wavelength range, we cannot determine the properties of this inner component, and thus we did not include it in our model.

The disk inclination (angle between the rotation axis and the line-of-sight) and PA were fitted by exploring different values, assuming as an initial guess that the disk lies in the B and A/C orbital plane ( $i = 47^\circ$ ; Carrasco-González et al. in preparation) and is perpendicular to the direction of the observed collimated jet (Krist et al. 2008).

Hence, the main free parameters are the viscosity parameter,  $\alpha$ , the mass accretion rate in the disk,  $\dot{M}_{\text{disk}}$ , and the degree of settling,  $\epsilon$ . Planet-forming disks are expected to have dust populations highly settled onto the midplane (i.e., a low value of  $\epsilon$ , defined as the dust-to-gas ratio in the atmosphere relative to the total of the disk), so that planetesimals can grow through the aggregation of large grains. Thus, we explored low values of  $\epsilon$ ,  $0.001 \leq \epsilon \leq 0.1$ .

To analyze how the viscosity affects the gas and dust evolution, we have carried out gas-dust two fluid hydrodynamical simulations as in Zhu et al. (2012). With a large viscosity (e.g.,  $\alpha = 10^{-2}$ ), such a small disk evolves very fast. As shown in the right panel of Figure 2, the disk gas surface density decreases by 4 orders of magnitude within 0.1 Myr and all the dust drifts to the central star. With a smaller viscosity (e.g.,  $\alpha = 10^{-3}$  as shown in the left panel of Fig. 2),  $\sim 0.1 M_J$  mass planets are sufficient to produce a cavity which is almost two orders of magnitude deep. Thus, multiple planets could account for the observed cavity in XZ Tau B as long as the viscosity is small enough ( $\alpha \leq 10^{-3}$ ).

Simulations also show that accretion onto the planet creating the gap can account for up to 90% of  $\dot{M}_{\text{disk}}$  (Zhu et al. 2011) and would reduce the mass accretion rate onto the star,  $\dot{M}_*$ . Therefore, we explored values of  $\dot{M}_{\text{disk}}$  in the range  $\dot{M}_* < \dot{M}_{\text{disk}} < 10 \dot{M}_*$ , where  $\dot{M}_*$  is given in Table 1.

We have run a grid of 40 models with parameters in the above-mentioned ranges. Since we are interested in studying the capability of the disk to form planets, we have selected the model that fits the data with the highest allowed value for the viscosity parameter, which gives the lowest disk mass ( $9 M_J$ ). As we show in §4, even this low-mass disk is capable to form a planetary system. The parameters of this disk are given in Table 1.

The resulting SED, showing the separate contributions of the main components, is plotted in Figure 3a. The free-free contribution from the ionized jet has also been taken into account in the fit, showing that it is negligible in the mm range. A comparison of the observed and model intensity profiles along the major axis of the disk is shown in Figure 3b. Figure 3c shows the surface density and temperature model profiles. Figure 3d shows a CASA simulated image of the model emission at 1.3 mm as it would be observed with the same ALMA configuration as Figure 1. These figures show that the model reproduces the observations reasonably well. Thus, our results support the interpretation that XZ Tau B is associated with a dwarf transitional disk.

#### 4. Discussion

Modeling shows that the outer radius of the disk is 3.4 au and the radius of the central cavity is 1.3 au (Table 1). These radii are well constrained by the intensity profile and are much smaller than those of other transitional disks (typically  $\sim 50$ -100 au for the disk and  $\sim 15$ -70 au for the cavity; Andrews et al. 2011, Espaillat et al. 2014, Andrews 2015). Tidal interactions in a close binary are expected to truncate circumstellar disks to an outer radius  $\sim 1/3$  of the binary separation (Papaloizou & Pringle 1977). This has been observed in the L1551-IRS5 binary system of disks, each 10 au in radius (Rodríguez et al. 1998). Interestingly, the radius of the XZ Tau B disk is significantly smaller than the value of  $\sim 14$  au expected from tidal truncation, given the separation of  $\sim 42$  au between XZ Tau B and the A/C pair. A highly eccentric orbit could truncate the disk at a smaller radius, but the analysis of the relative positions of the stars over  $>20$  yr favors a nearly circular orbit (Carrasco-González et al. 2009, Carrasco-González et al. in preparation).

The reason for the small size of the XZ Tau B disk is uncertain. It is feasible that the disk was originally small; that simple tidal truncation models (Papaloizou & Pringle 1977) may not apply for the particular geometry of this disk and truncation occurs at a smaller scale; that the disk is outwardly truncated by a forming planet in an outer orbit (Osorio et al. 2014); or that the outer parts of the disk have been removed by other mechanisms (e.g., swept out by the sequence of expanding bubbles from the A/C stars; Krist et al. 2008). It is possible that the gas component of the XZ Tau B disk is more extended than the dust, as it occurs in standard disks (e.g., HD 163296; de Gregorio-Monsalvo et al. 2013). Unfortunately, the sensitivity of our line observations is insufficient to set a tight constraint to the gas disk size. Anyhow, the disk of dust in XZ Tau B is much smaller than any other angularly resolved disk of dust imaged so far.

The observed image (Fig. 1a) is marginally asymmetric, with the flux density in the

southeast region  $\sim 30\%$  higher than in the northwest one. Such an asymmetry could not result from opacity effects due to the disk inclination since our modeled image (Figs. 3b, 3d) is symmetric. Instead, this asymmetry is suggestive of a dust trap, where the largest dust grains accumulate (e.g., Birnstiel et al. 2013, van der Marel et al. 2013). However, this needs to be confirmed with higher sensitivity data.

These results suggest that XZ Tau B shows the features that characterize transitional disks, but on a much smaller scale (e.g., compare Fig. 1a with Fig. 1b in Osorio et al. 2014). Since the evolution of these features is determined by their orbital motions around the central star, a dwarf disk like XZ Tau B is expected to evolve  $\sim 50$ -500 times faster than their bigger counterparts. Unfortunately, the current 1.3 mm ALMA observations, spanning just one week, are insufficient to search for disk evolution, but significant changes can occur in observations separated by only a few months. Thus, we anticipate that the disk in XZ Tau B, and possibly other similar dwarf disks, may serve in the near future as valuable small-scale models for a fast and efficient study of the evolution of transitional disks.

The diversity of planetary systems observed in the exoplanet surveys suggests that an equivalent diversity should be found in their progenitors, the protoplanetary disks. In particular, the Kepler mission has identified a number of “low-mass compact multiple-planet systems”, orbiting within  $< 1$  au from the star and with planetary masses ranging from a fraction to a few times the Earth’s mass (Lissauer et al. 2011, 2014, Jontof-Hutter et al. 2015). Dwarf disks similar to that found in XZ Tau B appear as the natural precursors of these systems.

To fit both the relatively high mm flux density of the disk and its small size, a high mass accretion rate was needed in our model. This, combined with the low viscosity of the disk, resulted in very high disk surface densities (Fig. 3c). These values are higher than those expected at the inner regions of larger disks around this type of stars (Williams & Cieza 2011, Andrews 2015) but they are still one order of magnitude smaller than the values of the “minimum mass protoplanetary nebula” estimated by Swift et al. (2013) to form “in situ” the Kepler-32 planetary system.

It is also interesting to compare with the compact system of five sub-Earth radius planets around the K0 star Kepler-444A, in a hierarchical triple stellar system. Dupuy et al. (2016) estimated a small radius of  $\sim 2$  au and a relatively large mass  $\gtrsim 70 M_J$  for the primordial protoplanetary disk around Kepler-444A. These authors propose that the outer regions of such a massive disk would have been unstable, leading to the formation of the triple star system through gravitational fragmentation. XZ Tau B could be similar to Kepler-444A. However, the disk of XZ Tau B presents a central gap, while the planets around Kepler-444A have masses well below the gap-opening mass (Dupuy et al. 2016). This implies that the

planets recently formed in XZ Tau B are probably more massive than the planets around Kepler-444A. The reason of this could be the difference in the position of the snowline. Whereas the whole disk of Kepler-444A would have fallen within its snowline, our model of XZ Tau B shows that (for points slightly above the disk midplane, where the minimum temperature is reached) it could be located inside the cavity, at a radius of  $\sim 0.5$  au, where  $T_{\min} = 180$  K (Fig. 3c). Therefore, giant planets, which form much more easily beyond the snowline (e.g., Ros & Johansen 2013), could be forming in the XZ Tau B disk cavity.

Some theoretical studies already pointed to the possible existence of a relatively large population of very small disks (McClure et al. 2008, Piétu et al. 2014, Kraus et al. 2015, Furlan et al. 2016). However, none of these putative dwarf disks has been angularly resolved. In XZ Tau B we have been able, not only to angularly resolve the disk and determine its size, but also to observe and model its substructure at au-scales. The Kepler mission raised a number of puzzling questions regarding the observed planetary systems at distances  $< 1$  au from the star, such as the debate of migration versus “in situ” planetary formation (Ogihara et al. 2015), or the abundance of super-Earths very close to the star (Lee et al. 2014). XZ Tau B opens a new window to investigate with ALMA observations the disk evolution and first stages of planet formation on time-scales and at radii that so far remained unexplored.



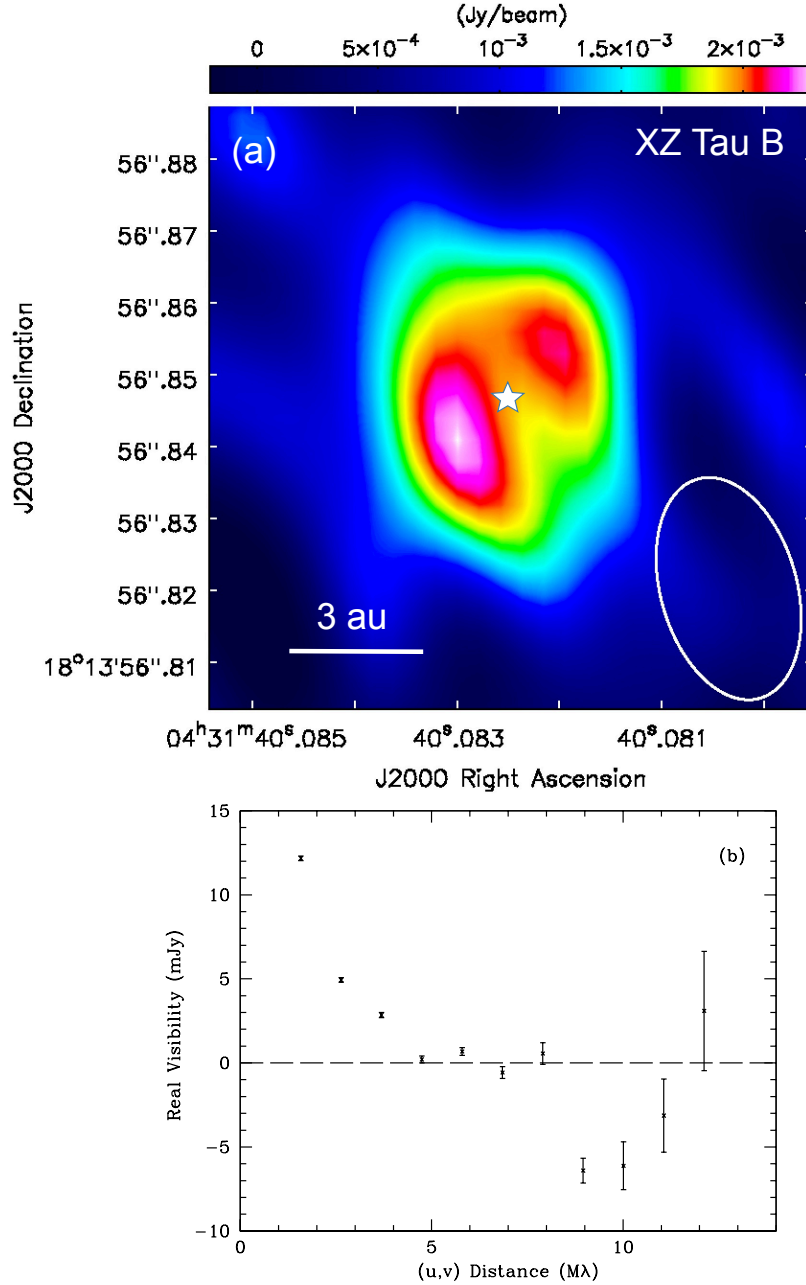


Fig. 1.— (a) ALMA image at 1.3 mm (robust=0, rms=0.28 mJy beam<sup>-1</sup>) of the disk of dust around XZ Tau B (indicated by a star, at  $\alpha(\text{J2000})=4^{\text{h}}31^{\text{m}}40.0825^{\text{s}}$ ,  $\delta(\text{J2000})=18^{\circ}13'56.847''$ ). The synthesized beam ( $0.032'' \times 0.019''$ , PA=16°) is shown in the lower-right corner. The intensity decrease in the northeast and southwest edges is an observational effect due to the beam elongation along this direction (see Osorio et al. 2014). (b) Azimuthally averaged visibility profile plotted in  $\sim 1 M\lambda$  bins.

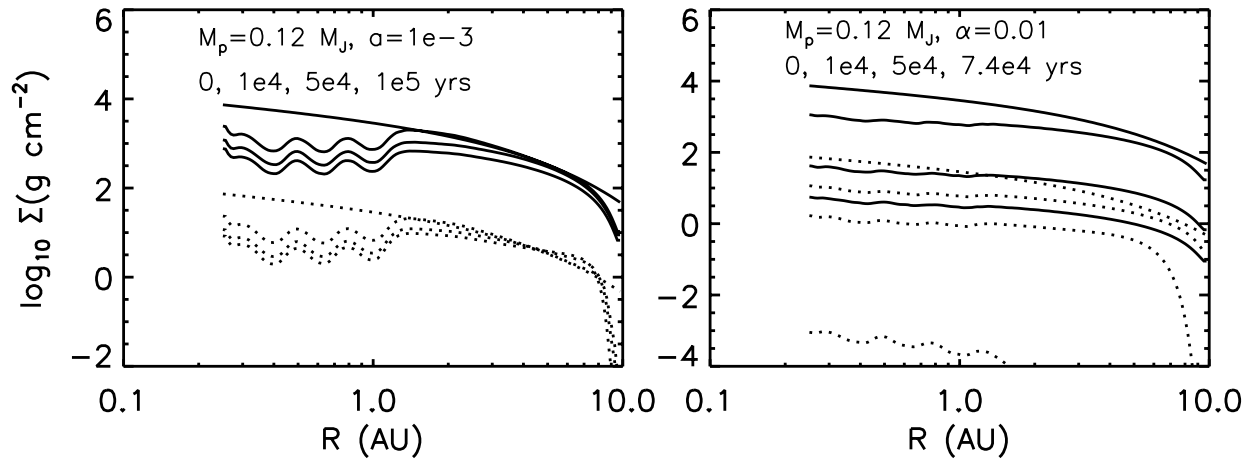


Fig. 2.— Hydrodynamical simulations of the surface density (solid line=gas; dotted line=1 mm dust) at different times for viscous disks ( $\alpha=0.001$ , left;  $\alpha=0.01$ , right) with three accreting  $0.12 M_J$  planets, at radii 0.4, 0.63, and 1 au.

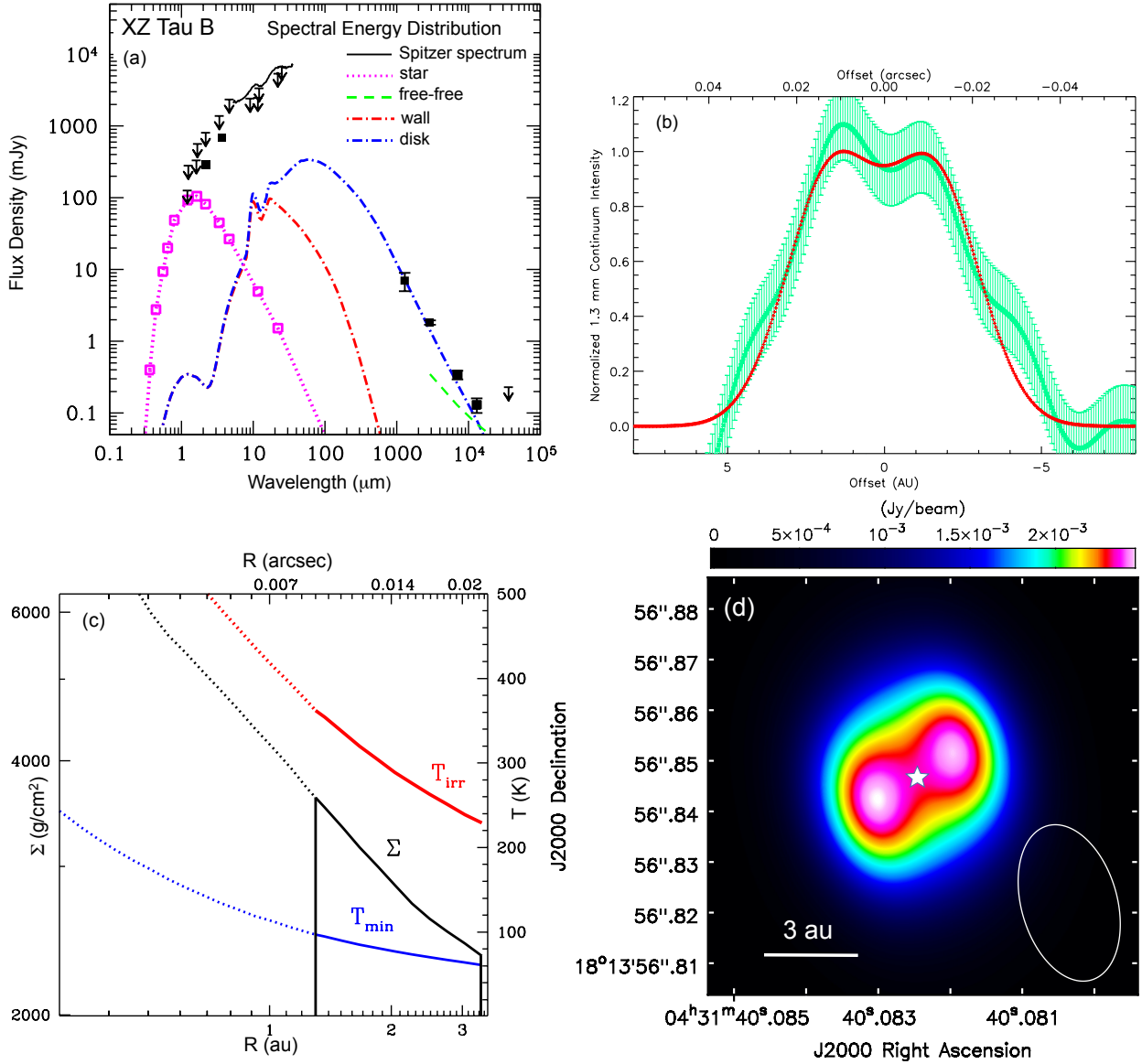


Fig. 3.— (a) Spectral energy distribution. Solid square symbols and continuous line are observational data. Arrows are upper limits, corresponding to data that do not separate XZ Tau B from A/C components. Open squares represent the calculated contribution of the star (see text). Discontinuous lines represent the model results. (b) Observed (green line with 1- $\sigma$  error bars) and model (red line) normalized intensity profile along a line passing through the two maxima (PA=126 $^\circ$ ) of the disk (positive offsets to the east). (c) Model surface density ( $\Sigma$ ), irradiation temperature ( $T_{\text{irr}}$ ), and minimum temperature ( $T_{\text{min}}$ ) radial distributions. (d) CASA simulated image of the 1.3 mm model emission, assuming the same antenna configuration as in Figure 1a.

Table 1. Parameters of the XZ Tau B Star and Disk

Parameter	Value	Notes	Refs.
Star			
Distance (pc)	140	Adopted	1
Visual Extinction (mag)	1.4	Adopted	2
Spectral Type	M2	Adopted	2
Age (Myr)	4.6	Adopted	2
Effective Temperature (K)	3550	Adopted	2
Radius ( $R_{\odot}$ )	1.24	Calculated	
Mass ( $M_{\odot}$ )	0.37	Adopted	2
Mass Accretion Rate ( $M_{\odot} \text{ yr}^{-1}$ )	$1.4 \times 10^{-8}$	Calculated	
Disk			
Inclination Angle (deg)	$35 \pm 10$	Adopted/Refined	3
Position Angle of Major Axis (deg)	$140 \pm 10$	Adopted/Refined	4
Inner Radius (au)	$1.30 \pm 0.05$	Fitted	
Outer Radius (au)	$3.4 \pm 0.1$	Fitted	
Viscosity Parameter	0.001	Adopted	
Mass Accretion Rate ( $M_{\odot} \text{ yr}^{-1}$ )	$7.0 \times 10^{-8}$	Fitted	
Degree of Settling	0.10	Fitted	
1.3 mm Optical Depth at 1 au	18	Calculated	
1.3 mm Optical Depth at 3.4 au	14	Calculated	
Mass Evacuated in Cavity ( $M_J$ )	3	Calculated	
Total Mass ( $M_J$ )	9	Calculated	
Dust Mass ( $M_{\oplus}$ )	25	Calculated	
Cavity Wall			
Radius (au)	$1.30 \pm 0.05$	= Disk Inner Radius	
Temperature (K)	420	Calculated	
Height (au)	0.09	= Disk Hydrostatic Scale Height	

References. — (1) Torres et al. 2009; (2) Hartigan & Kenyon 2003; (3) Carrasco-González et al. in preparation (4) Krist et al. 2008

Support from MINECO-FEDER AYA2014-57369-C3 grant, CONACyT, and DGAPA-UNAM is acknowledged. This paper makes use of the following ALMA data: ADS/JAO.ALMA#2011.0.000 ALMA is a partnership of ESO (representing its member states), NSF (USA) and NINS (Japan), together with NRC (Canada), NSC and ASIAA (Taiwan), and KASI (Republic of Korea), in cooperation with the Republic of Chile. The Joint ALMA Observatory is operated by ESO, AUI/NRAO and NAOJ. The National Radio Astronomy Observatory is a facility of the National Science Foundation operated under cooperative agreement by Associated Universities, Inc.

*Facilities:* ALMA

## REFERENCES

- ALMA Partnership, Brogan, C. L., Pérez, L. M., et al. 2015, *ApJ*, 808, L3 (AP2015a)
- ALMA Partnership, Fomalont, E. B., Vlahakis, C., et al. 2015, *ApJ*, 808, L1 (AP2015b)
- Andrews, S. M. 2015, *PASP*, 127, 961
- Andrews, S. M., Wilner, D. J., Espaillat, C., et al. 2011, *ApJ*, 732, 42
- Andrews, S. M., Wilner, D. J., Hughes, A. M., Qi, C., & Dullemond, C. P. 2009, *ApJ*, 700, 1502
- Birnstiel, T., Dullemond, C. P., & Pinilla, P. 2013, *A&A*, 550, L8
- Blum, J., & Wurm, G. 2008, *ARA&A*, 46, 21
- Calvet, N., D’Alessio, P., Watson, D. M., et al. 2005, *ApJ*, 630, L185
- Calvet, N., & Gullbring, E. 1998, *ApJ*, 509, 802
- Carrasco-González, C., Rodríguez, L. F., Anglada, G., & Curiel, S. 2009, *ApJ*, 693, L86
- Coffey, D., Downes, T. P., & Ray, T. P. 2004, *A&A*, 419, 593
- D’Alessio, P., Calvet, N., Hartmann, L., Franco-Hernández, R., & Servín, H. 2006, *ApJ*, 638, 314
- D’Alessio, P., Hartmann, L., Calvet, N., et al. 2005, *ApJ*, 621, 461
- de Gregorio-Monsalvo, I., Ménard, F., Dent, W., et al. 2013, *A&A*, 557, A133

- Dupuy, T. J., Kratter, K. M., Kraus, A. L., et al. 2016, *ApJ*, 817, 80
- Dzib, S. A., Loinard, L., Rodríguez, L. F., Galli, P. 2014, *ApJ*, 788, 162
- Espaillet, C., Calvet, N., Luhman, K. L., Muzerolle, J., & D’Alessio, P. 2008, *ApJ*, 682, L125
- Espaillet, C., Muzerolle, J., Najita, J., et al. 2014, *Protostars and Planets VI*, 497
- Forgan, D., Ivison, R. J., Sibthorpe, B., Greaves, J. S., & Ibar, E. 2014, *MNRAS*, 439, 4057
- Furlan, E., Fischer, W. J., Ali, B., et al. 2016, *ApJS*, 224, 5
- Hartigan, P., & Kenyon, S. J. 2003, *ApJ*, 583, 334
- Hioki, T., Itoh, Y., Oasa, Y., et al. 2009, *PASJ*, 61, 1271
- Hughes, A. M., Wilner, D. J., Calvet, N., et al. 2007, *ApJ*, 664, 536
- Jontof-Hutter, D., Rowe, J. F., Lissauer, J. J., Fabrycky, D. C., & Ford, E. B. 2015, *Nature*, 522, 321
- Kenyon, S. J., & Hartmann, L. 1995, *ApJS*, 101, 117
- Kraus, A. L., Andrews, S. M., Bowler, B. P., et al. 2015, *ApJ*, 798, L23
- Krist, J. E., Stapelfeldt, K. R., Hester, J. J., et al. 2008, *AJ*, 136, 1980
- Lee, E. J., Chiang, E., & Ormel, C. W. 2014, *ApJ*, 797, 95
- Lissauer, J. J., Dawson, R. I., & Tremaine, S. 2014, *Nature*, 513, 336
- Lissauer, J. J., Fabrycky, D. C., Ford, E. B., et al. 2011, *Nature*, 470, 53
- McClure, M. K., Espaillet, C., Calvet, N., et al. 2015, *ApJ*, 799, 162
- McClure, M. K., Forrest, W. J., Sargent, B. A., et al. 2008, *ApJ*, 683, L187
- Ogihara, M., Morbidelli, A., & Guillot, T. 2015, *A&A*, 578, A36
- Osorio, M., Anglada, G., Carrasco-González, C., et al. 2014, *ApJ*, 791, L36
- Papaloizou, J. C. B., Nelson, R. P., Kley, W., Masset, F. S., & Artymowicz, P. 2007, *Protostars and Planets V*, 655
- Papaloizou, J., & Pringle, J. E. 1977, *MNRAS*, 181, 441

- Pecaut, M. J., & Mamajek, E. E. 2013, *ApJS*, 208, 9
- Piétu, V., Guilloteau, S., Di Folco, E., Dutrey, A., & Boehler, Y. 2014, *A&A*, 564, A95
- Rodríguez, L. F., D’Alessio, P., Wilner, D. J., et al. 1998, *Nature*, 395, 355
- Ros, K., Johansen, A. 2013, *A&A*, 552, A137
- Sandell, G., & Aspin, C. 1998, *A&A*, 333, 1016
- Siess, L., Dufour, E., & Forestini, M. 2000, *A&A*, 358, 593
- Swift, J. J., Johnson, J. A., Morton, T. D., et al. 2013, *ApJ*, 764, 105
- Torres, R. M., Loinard, L., Mioduszewski, A. J., & Rodríguez, L. F. 2009, *ApJ*, 698, 242
- van der Marel, N., van Dishoeck, E. F., Bruderer, S., et al. 2013, *Science*, 340, 1199
- White, R. J., & Ghez, A. M. 2001, *ApJ*, 556, 265
- Williams, J. P., & Cieza, L. A. 2011, *ARA&A*, 49, 67
- Zapata, L. A., Galván-Madrid, R., Carrasco-González, C., et al. 2015, *ApJ*, 811, L4
- Zhu, Z., Nelson, R. P., Dong, R., Espaillat, C., & Hartmann, L. 2012, *ApJ*, 755, 6
- Zhu, Z., Nelson, R. P., Hartmann, L., Espaillat, C., & Calvet, N. 2011, *ApJ*, 729, 47